Theory of Sidebands of the *U*-Center Vibrations in Alkali Halides: An Extended Model*

T. Gethins, T. Timusk,† and E. J. Woll, Jr.
McMaster University, Hamilton, Ontario, Canada
(Received 12 December 1966)

The substitutional H^--ion impurity in alkali halide crystals gives rise to a sharp vibrational local mode at high frequency. Sidebands of this vibrational mode, caused by anharmonic interaction, reflect with some distortion the density of phonon states as perturbed by the presence of the impurity. The recent model of Timusk and Klein for this perturbation has been extended to account for the distortion of the crystal near the H^- ion. The sideband spectrum is calculated for KBr and KI, using a Green's-function method. The agreement with experiment is greatly improved. In particular, the extended theory predicts resonances at the top of the acoustic band for both crystals, a resonance at the bottom of the optical band for KBr, and a resonance in the band gap for KI, all of which accord with experimental observation.

I. INTRODUCTION

ALKALI halide crystals containing *U* centers (substitutional H^- impurities) have for some time been known to have a high-frequency localized vibrational mode. This mode is optically active in the infrared region, and was first observed by Schaefer.[1] The frequency of the local mode is determined by the small mass of the H^- ion, as compared to the host ion,[2–4] and by a reduction in force constant connecting the H^- ion to its nearest neighbors, amounting, typically, to 50% of the nearest-neighbor force constant in the perfect host lattice.[5,6]

Sidebands of the local mode vibrations have also been observed[1,7,8] and have, to some extent, been theoretically investigated.[7,9] The existence of sidebands is basically due to the anharmonic coupling of the local mode vibration to other vibrational modes of the crystal. The cubic anharmonic coupling dominates[7–9] and the sideband spectrum reflects—with distortions of shape caused by the highly localized nature of the coupling—the vibration spectrum of the crystal.

Timusk and Klein[9] have developed a theory which attempts to explain the shape of the sideband spectrum in terms of the anharmonic coupling of the H^- ion to its nearest neighbors. The sideband spectrum is calculated, to lowest order in the anharmonic coupling constant, taking into account the effect of the *U* center on the harmonic vibrational spectrum of the crystal. Nguyen[10] has performed a similar calculation, giving a careful account of the interaction which produces the sideband, including the possibilities both of anharmonic and second-order electric-dipole interaction. He finds the anharmonic interaction to be the dominant mechanism, thereby justifying the use of this interaction by Timusk and Klein and in the present paper.

The experimental and theoretical results of Timusk and Klein are given in Figs. 4 and 5 for KBr [9] and KI.[11] The Timusk-Klein model (hereafter called the TK model) satisfactorily reproduces the general shape of the experimental results, including especially the shape and spacing of the peaks in the acoustic band of KBr. This agreement was achieved without the use of any parameter fitted to sideband shape, the single relevant parameter of the model—the nearest-neighbor force constant—being fitted to the local mode frequency.

However, certain predictions of the TK model are not in agreement with the experimental curves. In particular, the model predicts for the sideband spectrum a large spike, in the band gap between acoustic and optical bands of the perfect crystal. This spike is not observed experimentally in the case of KBr, though a spike at 93.5 cm^{-1} does appear in the data for KI. Moreover, the TK model fails to predict a shoulder in the peak at the top of the acoustic band in KBr, which appears as a second peak in KI. Third, the TK model predicts a resonance in the optical band for both KBr and KI, which fails to appear in experimental data. This resonance is particularly sharp in KI.

It will be shown in the present work that these three unsatisfactory features of the TK model can be eliminated by extending the model to allow for additional perturbation of the harmonic lattice modes by the presence of the impurity. In Sec. II of this paper, the general formalism is reviewed. In Sec. III, the extended model of the *U* center is introduced. In Sec. IV, the sideband spectrum of the local mode vibration is calculated for the cases of KBr and KI. In Sec. V, the results are presented and discussed.

* Research supported by the National Research Council of Canada.
† Alfred P. Sloan Fellow.
[1] G. Schaefer, J. Phys. Chem. Solids **2**, 233 (1960).
[2] H. Rosenstock and C. Klick, Phys. Rev. **119**, 1198 (1960).
[3] R. Wallis and A. Maradudin, Progr. Theoret. Phys. (Kyoto) **24**, 1055 (1960).
[4] S. Takeno, S. Kashirvamura, and E. Tenamoto, Progr. Theoret. Phys. (Kyoto) Suppl. **23**, 124 (1962).
[5] S. S. Jaswal and D. J. Montgomery, Phys. Rev. **135**, A1257 (1964).
[6] R. Fieschi, G. F. Nardelli, and N. Terzi, Phys. Letters **12**, 290 (1964); R. Fieschi, G. N. Nardelli, and N. Terzi, Phys. Rev. **138**, A203 (1965).
[7] B. Fritz, U. Gross, and D. Bäuerle, Phys. Status Solidi **11**, 231 (1965).
[8] Y. Brada and S. S. Mitra, Bull. Am. Phys. Soc. **9**, 644 (1964).
[9] T. Timusk and M. V. Klein, Phys. Rev. **141**, 664 (1966).
[10] Nguyen Yuan Xinh, Solid State Commun. 4, 9 (1966).
[11] T. Timusk and M. V. Klein (to be published).

II. CALCULATION OF THE LINE SHAPE

In the present paper, a matrix notation will be used.[12] Thus, the eigenfrequencies and eigenmodes of the alkali halide crystal, including a U center, are given by the solutions of the matrix equation

$$(\bar{A}-\omega^2 1)u=0, \tag{1}$$

where ω is the frequency of vibration. The dynamical matrix $\bar{A}$, can conveniently be defined in the representation whose rows and columns are labeled by position of the ion $\mathbf{L}$, direction of displacement α, and type of ion κ ($\kappa=+$ and $\kappa=-$, indicating alkali and halide ions, respectively). The elements of $\bar{A}$ are defined as derivatives of the potential energy V of the crystal by

$$\bar{A}_{\mathbf{L}\mathbf{L}'}{}^{\alpha\kappa,\alpha'\kappa'}=[\partial^2 V/\partial u_{\mathbf{L}}{}^{\alpha\kappa}\partial u_{\mathbf{L}'}{}^{\alpha'\kappa'}]_{u=0} +\lambda\omega^2\delta_{\mathbf{L},0}\delta_{\mathbf{L},\mathbf{L}'}\delta_{\alpha,\alpha'}\delta_{\kappa,-}\delta_{\kappa,\kappa'}. \tag{2}$$

The variables $u_{\mathbf{L}}{}^{\alpha\kappa}$ are elements (in the $\mathbf{L}\kappa\alpha$ representation) of the vector u. The element $u_{\mathbf{L}}{}^{\alpha\kappa}$ is given by the $\mathbf{L}\kappa\alpha$th component of the ionic displacement multiplied by $\sqrt{M_\kappa}$, where M_κ is the mass of the ion of type κ in the perfect lattice. The light mass of the H^- ion is accounted for by the $\lambda\omega^2$ term, where λ is given by

$$\lambda=(M_- - M_H)/M_-, \tag{3}$$

with M_H the mass of the H^- ion.

The Green's-function matrix $\bar{G}(\omega^2)$ of the lattice including U center is defined by the matrix equation.

$$(\bar{A}-\omega^2 1)\bar{G}(\omega^2)=1. \tag{4}$$

In the representation in which $\bar{A}$ is diagonal, which will be called the l representation, the diagonal elements of $\bar{A}$ are $\omega_l{}^2$, the eigenfrequencies of the crystal. In this representation, $\bar{G}$ is also diagonal. From Eq. (4), its elements are

$$\bar{G}_{ll'}(\omega^2)=\delta_{ll'}/(\omega_l{}^2-\omega^2). \tag{5}$$

The dynamical matrix $\bar{A}$ can be written in the form

$$\bar{A}=A+\Gamma, \tag{6}$$

where A is the dynamical matrix of the perfect alkali halide crystal and Γ is the change resulting from introduction of the H^- ion. It is useful to define the Green's-function matrix for the perfect crystal, $G(\omega^2)$, by the matrix equation

$$(A-\omega^2 1)G(\omega^2)=1. \tag{7}$$

Using Eq. (7) with Eq. (4) and Eq. (6), $\bar{G}(\omega^2)$ can be written

$$\bar{G}(\omega^2)=[1+G(\omega^2)\Gamma]^{-1}G(\omega^2). \tag{8}$$

The anharmonic coupling between the local mode and other vibrations of the crystal arises primarily from the anharmonic connection of the H^- ion to its nearest neighbors.[9] The formula for the upper sideband line shape for radiation polarized in the x direction is

$$I^+(\omega)=(\hbar B^2/4\pi M_H{}^2\omega^2\Omega^2)\tilde{X}\,\mathrm{Im}\{\bar{G}(\omega^2+i0^+)\}X, \tag{9}$$

where $I^+(\omega)$ is the power absorbed as a function of frequency ω, measured with respect to the local mode frequency Ω. B is the relevant anharmonic coupling constant, and the imaginary part of the Green's-function matrix is to be taken for the variable ω^2 just above the real ω^2 axis. The vector X (and its adjoint $\tilde{X}$) has, in the $\mathbf{L}\kappa\alpha$ representation, only two nonzero elements:

$$X_{\mathbf{L}}{}^{\alpha\kappa}=(2M_+)^{-1/2}(\delta_{\mathbf{L},a\bar{x}}-\delta_{\mathbf{L},-a\bar{x}})\delta_{\kappa,+}\delta_{\alpha,x}, \tag{10}$$

where a is the nearest-neighbor distance and $\bar{x}$ is the unit vector in the x direction. The restriction of X to two elements results essentially from the use of nearest-neighbor anharmonic forces. Only the even combination of nearest-neighbor displacements has been taken, since odd motions exert no net (cubic) anharmonic force on the H^- ion.

Using Eq. (8), the formula for the line shape can be written

$$I^+(\omega)=(\hbar B^2/4\pi M_H{}^2\omega^2\Omega^2)\tilde{X} \times\mathrm{Im}\{[1+G(\omega^2+i0^+)\Gamma]^{-1}G(\omega^2+i0^+)\}X. \tag{11}$$

The vector X and the matrices G and Γ can be treated in any representation. In particular, the representation which diagonalizes Γ will be found to simplify the calculations. The nature of the matrix Γ is the subject of the next section.

III. THE EXTENDED MODEL OF THE U CENTER

The TK model accounts for harmonic perturbation of the crystal by the H^- ion by changing the force constants between the H^- ion and its nearest neighbors, in addition to the mass change. These are the only effects which prove to be important in determining the vibration frequency of the local mode. However, the perturbation of the crystal by the H^- ion is certainly more extensive than this. Measurements of volume change of a KBr crystal with increasing concentration of U centers[13] show that a volume shrinkage of order 10% can be expected in the vicinity of the H^- ion. The occurrence of this shrinkage implies that the H^- ion has a smaller ionic radius than the halide ion it replaces, that is, the neighbors of the H^- ion move in until they feel an exchange repulsion which balances what they feel from other neighbors. Because the forces between ions are not perfectly harmonic, this change of position results in a change of force constants. The change will be largest (apart from the change between the H^- ion and its nearest neighbors) for the interionic distances which are most stretched; namely, between the nearest neighbors of the H^- ion and their nearest neighbors in

[12] See, for example, the article by A. A. Maradudin, in *Astrophysics and the Many-Body Problem* edited by K. W. Ford (W. A. Benjamin Inc., New York, 1963).

[13] R. Hilsch and R. W. Pohl, Trans. Faraday Soc. 34, 883 (1938).

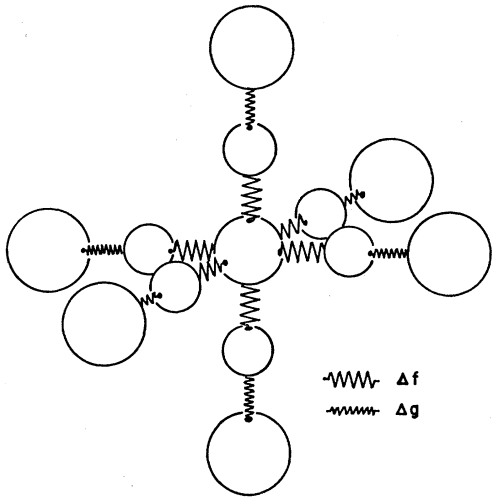

FIG. 1. The "molecule" of force-constant changes introduced by insertion of the H^- ion. The ion at the center is the H^-. Its first-neighbor (alkali) atoms are shown, as well as its fourth-neighbor (halide) atoms. The spring constant Δf is determined by the local mode frequency; the spring constant Δg is an adjustable parameter of the present theory.

the direction away from the H^- ion. (These are fourth neighbors to the H^- ion; see Fig. 1.)

The change in force constants coupling the H^- ion to its second and third neighbors can be expected to be small, because these force constants are themselves small.

The change in potential energy is then taken to be simply

$$\Delta V=\sum_{\substack{\alpha=1,3\\ s=\pm 1}}[(\Delta f/2)(M_+^{-1/2}u_{sa\bar{\alpha}}{}^{\alpha+}-M_-^{-1/2}u_0{}^{\alpha-})^2 +(\Delta g/2)(M_-^{-1/2}u_{2sa\bar{\alpha}}{}^{\alpha-}-M_+^{-1/2}u_{sa\bar{\alpha}}{}^{\alpha+})^2], \quad (12)$$

where Δf has been taken as the change of force constant between the H^- ion and its nearest neighbors, while Δg has been taken as the change of force constant between the nearest neighbors and the fourth neighbors, and $\bar{\alpha}$ is the unit vector in the direction α. The pairs of ions affected by the sum in Eq. (12), and the corresponding force constant changes, are shown in Fig. 1.

The matrix Γ can be constructed, in the $\mathbf{L}\kappa\alpha$ representation, by taking appropriate derivatives of the potential energy. [See Eq. (2).] The only nonzero elements of Γ are

$$\begin{aligned}
\Gamma_{0,0}{}^{\alpha-,\alpha-}&=2\Delta f/M_-+\lambda\omega^2=b_1,\\
\Gamma_{\pm a\bar{\alpha},\pm 2a\bar{\alpha}}{}^{\alpha+,\alpha-}&=-\Delta g/(M_+M_-)^{1/2}=b_2,\\
\Gamma_{\pm a\bar{\alpha},\pm a\bar{\alpha}}{}^{\alpha+,\alpha+}&=(\Delta f+\Delta g)/M_+=b_3,\\
\Gamma_{\pm 2a\bar{\alpha},\pm 2a\bar{\alpha}}{}^{\alpha-,\alpha-}&=\Delta g/M_-=b_4,\\
\Gamma_{\pm a\bar{\alpha},0}{}^{\alpha+,\alpha-}&=-\Delta f/(M_+M_-)^{1/2}=b_5.
\end{aligned} \quad (13)$$

In this representation, the matrix Γ can conveniently be written in the block form[14]

$$\Gamma=\left[\begin{array}{ccc|c} \Lambda_x & 0 & 0 & \\ 0 & \Lambda_y & 0 & 0 \\ 0 & 0 & \Lambda_z & \\ \hline & 0 & & 0 \end{array}\right], \quad (14)$$

where Λ_α is the matrix

$$\Lambda_\alpha=\begin{bmatrix} b_4 & b_2 & 0 & 0 & 0\\ b_2 & b_3 & b_5 & 0 & 0\\ 0 & b_5 & b_1 & b_5 & 0\\ 0 & 0 & b_5 & b_3 & b_2\\ 0 & 0 & 0 & b_2 & b_4 \end{bmatrix} \quad (15)$$

whose rows and columns are labeled by the αth component of the displacements of the ions at $-2a\bar{\alpha}$, $-a\bar{\alpha}$, 0, $a\bar{\alpha}$, and $2a\bar{\alpha}$.

It is useful to think of the nonzero part of Γ as the force constant matrix for a "molecule." The appropriate molecule is pictured in Fig. 1. The eigenvectors and eigenvalues which diagonalize Γ are just the normal modes and frequencies of this molecule. The form of Γ written in Eq. (14) indicates that the molecule is highly degenerate. Only the even modes of the molecule will be required for subsequent calculations (i.e., the modes in which the H^- ion does not move).

Each submatrix Λ_α has the same two even eigenmodes, labeled by e_1 and e_2, whose normalized eigenvectors have the elements

$$\begin{aligned}
q_L{}^{\alpha\kappa}(e_1)&=2^{-1/2}(1+b^2)^{-1/2}(b\delta_{L,2a\bar{\alpha}}\delta_{\kappa,-}+\delta_{L,a\bar{\alpha}}\delta_{\kappa,+}\\
&\quad -\delta_{L,-a\bar{\alpha}}\delta_{\kappa,+}-b\delta_{L,-2a\bar{\alpha}}\delta_{\kappa,-}), \quad (16)\\
q_L{}^{\alpha\kappa}(e_2)&=2^{-1/2}(1+b^2)^{-1/2}(-\delta_{L,2a\bar{\alpha}}\delta_{\kappa,-}+b\delta_{L,a\bar{\alpha}}\delta_{\kappa,+}\\
&\quad -b\delta_{L,-a\bar{\alpha}}\delta_{\kappa,-}+\delta_{L,-2a\bar{\alpha}}\delta_{\kappa,-}),
\end{aligned}$$

where b is given by

$$b=\{b_4-b_3-[(b_4-b_3)^2+4b_2^2]^{1/2}\}/2b_2. \quad (17)$$

In terms of these eigenvectors of Λ_α, the eigenvectors of Γ can be written

$$\begin{aligned}
Q_L{}^{\alpha\kappa}(1)&=3^{-1/2}(\delta_{\alpha,x}+\delta_{\alpha,y}+\delta_{\alpha,z})q_L{}^{\alpha\kappa}(e_1),\\
Q_L{}^{\alpha\kappa}(2)&=3^{-1/2}(\delta_{\alpha,x}+\delta_{\alpha,y}+\delta_{\alpha,z})q_L{}^{\alpha\kappa}(e_2),\\
Q_L{}^{\alpha\kappa}(3)&=6^{-1/2}(2\delta_{\alpha,x}-\delta_{\alpha,y}-\delta_{\alpha,z})q_L{}^{\alpha\kappa}(e_1),\\
Q_L{}^{\alpha\kappa}(4)&=6^{-1/2}(2\delta_{\alpha,x}-\delta_{\alpha,y}-\delta_{\alpha,z})q_L{}^{\alpha\kappa}(e_2),\\
Q_L{}^{\alpha\kappa}(5)&=2^{-1/2}(\delta_{\alpha,y}-\delta_{\alpha,z})q_L{}^{\alpha\kappa}(e_1),\\
Q_L{}^{\alpha\kappa}(6)&=2^{-1/2}(\delta_{\alpha,y}-\delta_{\alpha,z})q_L{}^{\alpha\kappa}(e_2).
\end{aligned} \quad (18)$$

The eigenvalue corresponding to modes 1, 3, and 5 is the eigenvalue of the e_1 mode,

$$e_1=\tfrac{1}{2}(b_4+b_3-[(b_4-b_3)^2+4b_2^2]^{1/2}), \quad (19)$$

[14] The first fifteen rows and columns of the representation have been taken to refer to the H^- ion and to the appropriate components of displacement of its nearest and fourth-nearest neighbors.

while that of modes 2, 4, and 6 is

$$e_2=\tfrac{1}{2}(b_4+b_3+[(b_4-b_3)^2+4b_2^2]^{1/2}). \quad (20)$$

Modes 1 and 2 have A_{1g} symmetry descriptively called "breathing" symmetry, while modes 3 and 4 and modes 5 and 6 have E_g and E_g' symmetry, respectively, called "tetragonal" symmetry. (See Ref. 9.)

In the evaluation of line shape it will be convenient to use the following representation, labeled by γ: The eigenvectors of Γ are used as a basis for the 15×15 subspace in which Γ has nonzero elements; the $\mathbf{L}\kappa\alpha$ representation is used elsewhere. In the γ representation, the vector X has only four elements, corresponding to the even eigenmodes of Γ whose eigenvectors are given in Eq. (18).

IV. CALCULATION OF THE SIDEBAND SPECTRUM

The formula for line shape in Eq. (11) requires evaluation of the scalar quantity

$$\begin{aligned}\tilde{X}\bar{G}X&=\tilde{X}(1+G\Gamma)^{-1}GX \quad (21)\\ &=\tilde{X}GX-\tilde{X}G\Gamma GX+\tilde{X}G\Gamma G\Gamma GX-\cdots,\end{aligned}$$

where a power-series expansion has been indicated. In the $\mathbf{L}\kappa\alpha$ representation, neither X nor Γ has elements apart from the 15×15 subspace in which Γ has nonzero elements. From Eq. (21), it is apparent that only the corresponding 15×15 elements of the matrix G will enter the evaluation of the quantity $\tilde{X}\bar{G}X$. Use of the γ representation further simplifies evaluation of Eq. (21). First, note that, by comparison of Eq. (10) and Eq. (18), X can be written in the form

$$\begin{aligned}X&=X_A+\sqrt{2}X_E,\\ X_A&=[3M_+(1+b^2)]^{-1/2}[Q(1)+bQ(2)], \quad (22)\\ X_E&=[3M_+(1+b^2)]^{-1/2}[Q(3)+bQ(4)].\end{aligned}$$

The components of the vectors $Q(\gamma)$ are given in Eq. (18). Viewed in the γ representation, therefore, the vector X has only four nonzero elements, all referring to modes of even symmetry, two of which refer to modes of breathing symmetry A_{1g} and two to modes of tetragonal symmetry E_g. Moreover, the matrix G can have no elements $G_{\gamma\gamma'}$ unless γ and γ' refer to modes of the same symmetry, since G is the Green's function for a lattice of full octahedral symmetry.

Therefore, the scalar quantity $\tilde{X}\bar{G}X$ can be written in the form

$$\tilde{X}\bar{G}X=\tilde{X}_A\bar{G}X_A+2\tilde{X}_E\bar{G}X_E, \quad (23)$$

and the evaluation of either quantity requires only the inversion of a two-by-two matrix.

It is therefore necessary to know, of the matrix G, only the elements of two 2×2 submatrices. The shell model VI of Cowley *et al.*[15] was used to calculate the eigenfrequencies and polarization vectors for the perfect lattice. The matrix elements $G_{\gamma\gamma'}$ can be written

$$G_{\gamma\gamma'}=\sum_{\mathbf{k},\lambda} T_{\gamma,\mathbf{k}\lambda}(\omega_{\mathbf{k}\lambda}^2-\omega^2)^{-1}T_{\mathbf{k}\lambda,\gamma'}, \quad (24)$$

where the sum runs over the eigenvectors $\mathbf{k}$ and polarization branches λ of the perfect lattice, and the $\omega_{\mathbf{k}\lambda}$ are the eigenfrequencies of the lattice. The required elements of the transformation matrix $T_{\gamma,\mathbf{k}\lambda}$ are

$$\begin{aligned}
T_{1,\mathbf{k}\lambda}&=(i/\sqrt{N})\sum_{\alpha=1,3}[\epsilon_\alpha^+(\mathbf{k},\lambda)\sin k_\alpha a+b\epsilon_\alpha^-(\mathbf{k},\lambda)\sin 2k_\alpha a],\\
T_{2,\mathbf{k}\lambda}&=(i/\sqrt{N})\sum_{\alpha=1,3}[b\epsilon_\alpha^+(\mathbf{k},\lambda)\sin k_\alpha a-\epsilon_\alpha^-(\mathbf{k},\lambda)\sin 2k_\alpha a],\\
T_{3,\mathbf{k}\lambda}&=(i/\sqrt{N})\sum_{\alpha=1,3}[\epsilon_\alpha^+(\mathbf{k},\lambda)\sin k_\alpha a+b\epsilon_\alpha^-(\mathbf{k},\lambda)\sin 2k_\alpha a](3\delta_{\alpha,x}-1),\\
T_{4,\mathbf{k}\lambda}&=(i/\sqrt{N})\sum_{\alpha=1,3}[b\epsilon_\alpha^+(\mathbf{k},\lambda)\sin k_\alpha a-\epsilon_\alpha^-(\mathbf{k},\lambda)\sin 2k_\alpha a](3\delta_{\alpha,x}-1),
\end{aligned} \quad (25)$$

where $\epsilon_\alpha^\kappa(\mathbf{k},\lambda)$ are the polarization vectors of the perfect lattice and N is the number of ions in the crystal. The sums on $\mathbf{k}$ and λ necessary in Eq. (24) are performed numerically. The matrix elements $G_{\gamma\gamma'}$ are most easily computed in terms of the function $I_{\gamma\gamma'}(\omega^2)$, defined by

$$I_{\gamma\gamma'}(\omega^2)=\mathrm{Im}\{G_{\gamma\gamma'}(\omega^2+i0^+)\}=\pi\textstyle\sum_{\mathbf{k},\lambda}T_{\gamma,\mathbf{k}\lambda}\delta(\omega_{\mathbf{k}\lambda}^2-\omega^2)T_{\mathbf{k}\lambda,\gamma'}. \quad (26)$$

The real part of $G_{\gamma\gamma'}$ can be found, using the Cauchy relations,[16] to be

$$R_{\gamma\gamma'}(\omega^2)=\mathrm{Re}\{G_{\gamma\gamma'}(\omega^2+i0^+)\}=\frac{1}{2\pi}\int_0^\infty\frac{I_{\gamma\gamma'}(s^2+i0^+)}{s^2-\omega^2-i0^+}d(s^2). \quad (27)$$

The integral is evaluated using a numerical procedure suggested by Maradudin.[17]

[15] R. A. Cowley, W. Cochran, B. N. Brockhouse, and A. D. B. Woods, Phys. Rev. **131**, 1030 (1963); A. D. B. Woods, W. Cochran, and B. N. Brockhouse, *ibid.* **119**, 980 (1960).
[16] E. G. Phillips, *Functions of a Complex Variable* (Oliver and Boyd, London, 1961), p. 93.
[17] A. J. Sievers, A. A. Maradudin, and S. S. Jaswal, Phys. Rev. **138**, A272 (1965).

The line shape can now be written in the form

$$l^+(\omega)=[\hbar B^2/12\pi M_+M_H{}^2\omega^2\Omega^2(1+b^2)](N_A/D_A+2N_E/D_E)\,, \tag{28}$$

where the numerators and denominators N_A, N_E, D_A, and D_E are given by

$$\begin{aligned}
N_A&=D_{RA}[I_{11}+2bI_{12}+b^2I_{22}+(e_2+b^2e_1)(R_{11}I_{22}+R_{22}I_{11}-2R_{12}I_{12})]\\
&\quad -D_{IA}[R_{11}+2bR_{12}+b^2R_{22}+(e_2+b^2e_1)(R_{11}R_{22}-I_{11}I_{22}-R_{12}{}^2+I_{12}{}^2)]\,,\\
D_A&=D_{RA}{}^2+D_{IA}{}^2\,,\\
D_{RA}&=1+e_1R_{11}+e_2R_{22}+e_1e_2(R_{11}R_{22}-I_{11}I_{22}-R_{12}{}^2+I_{12}{}^2)\,,\\
D_{IA}&=e_1I_{11}+e_2I_{22}+e_1e_2(R_{11}I_{22}+R_{22}I_{11}-2R_{12}I_{12})\,,\\
N_E&=D_{RE}[I_{33}+2bI_{34}+b^2I_{44}+(e_2+b^2e_1)(R_{33}I_{44}+R_{44}I_{33}-2R_{34}I_{34})]\\
&\quad -D_{IE}[R_{33}+2bR_{34}+b^2R_{44}+(e_2+b^2e_1)(R_{33}R_{44}-I_{33}I_{44}-R_{34}{}^2+I_{34}{}^2)]\,,\\
D_E&=D_{RE}{}^2+D_{IE}{}^2\,,\\
D_{RE}&=1+e_1R_{33}+e_2R_{44}+e_1e_2(R_{33}R_{44}-I_{33}I_{44}-R_{34}{}^2+I_{34}{}^2)\,,\\
D_{IE}&=e_1I_{33}+e_2I_{44}+e_1e_2(R_{33}I_{44}+R_{44}I_{33}-2R_{34}I_{34})\,.
\end{aligned} \tag{29}$$

The quantities $D_{RA}-iD_{IA}$ and $D_{RE}-iD_{IE}$ are just the determinants of the 2×2 submatrices of $1+G\Gamma$; these arise in the matrix inversion required to evaluate Eq. (21).

The appearance of in-band resonances or out-of band poles in the side band spectrum is governed by the behavior of D_{RA} and D_{RE}; a resonance or pole occurs where one of these is zero. The quantities D_{IA} and D_{IE} determine whether a zero of D_{RA} or D_{RE} will produce a resonance or a pole. Since these quantities are zero for ω^2 outside the acoustic or optical bands of the perfect crystal, but finite inside these bands, an in-band zero will produce a resonance of finite height in the sideband spectrum, while an out-of-band zero will produce a pole.[18] The quantities D_{RA} and D_{IA}, with D_{RE} and D_{IE}, are plotted in Figs. 2 and 3 for the cases of KBr and KI, respectively. It can be seen that in-band resonances are to be expected at 109 cm^{-1} (for the breathing mode) and at 78.5 cm^{-1} and, less sharply, at 118.5 cm^{-1} (for the tetragonal mode) in KBr. For KI, a pole is expected in the gap at 89.6 cm^{-1}, and an in-band resonance at 66.9 cm^{-1}.

The resulting sideband spectra are plotted in Figs. 4 and 5 for KBr and KI, respectively.

The force constants used are noted on the figures. They were determined as follows: Δf has the value given by Timusk and Klein.[9,11] As discussed by TK, the frequency of the local mode is determined, to a very good approximation, by the diagonal element of the matrix Γ corresponding to displacement of the H^- ion. This element is not affected by the change of Γ made in the present model. The values used for Δg were chosen to give a reasonable qualitative fit to the line shape data. As discussed in the next section, it is unrealistic

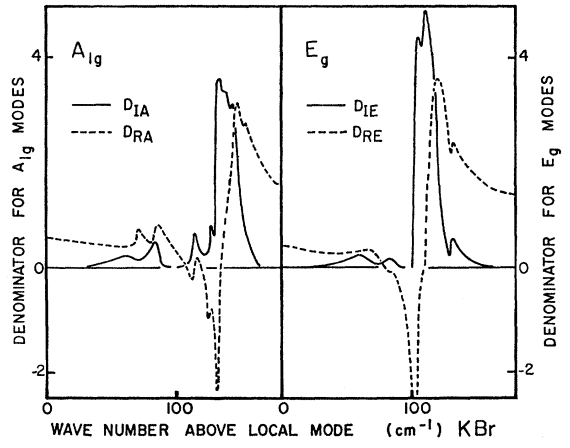

FIG. 2. The quantities D_{RA}, D_{IA}, D_{RE}, and D_{IE}, occurring in the resonance denominators of Eq. (28) are plotted for KBr as functions of wave number. "Breathing" and "tetragonal" resonances in the sideband spectrum occur where D_{RA} and D_{RE}, respectively, pass through zero with negative slope. The height of a resonance is determined by the value of D_{IA} or D_{IE} at the zero. A "tetragonal" resonance is predicted at 78.5 cm^{-1} and "breathing" resonances at 108 cm^{-1} and 118.5 cm^{-1}.

[18] Note that resonances occur only for those zeros of D_{RA} or D_{RE} for which the slope is negative.

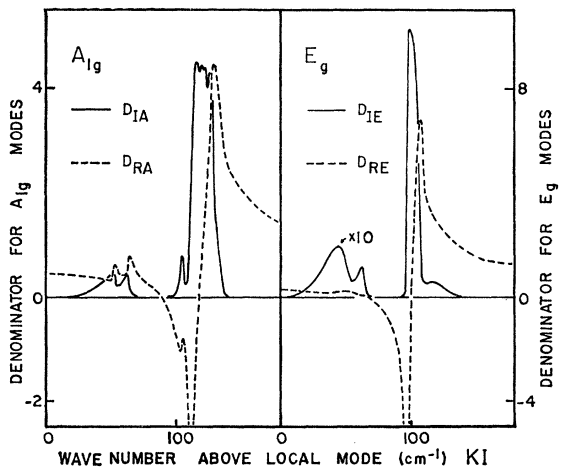

FIG. 3. The quantities D_{RA}, D_{IA}, D_{RE}, and D_{IE} are plotted for KI. (See caption, Fig. 2.) A "tetragonal" resonance is predicted at 67 cm^{-1} and a "breathing" resonance at 89.5 cm^{-1}, in the gap.

at the present time to try to perform fine adjustments on the setting of Δg.

The functions $I_{\gamma\gamma'}(\omega^2)$ were calculated using the shell-model parameters of Cowley *et al.*[15] for KBr and Dowling *et al.*[19] for KI. The mesh size used, following TK, effectively includes 64 000 points in the first Brillouin zone. The calculated eigenfrequencies and polarization vectors were sorted into 120 frequency "bins" each of size 0.05×10^{12} cps. For each point, the value of the product of the transformation matrix elements $T_{\gamma,k\lambda}$ was computed, and the total contribution

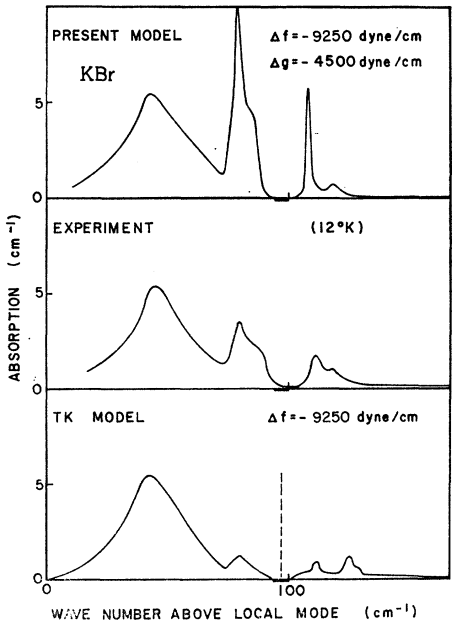

FIG. 4. The results of the present calculation for KBr are compared with experimental and theoretical results of Timusk and Klein (Ref. 9). The bar under the wave-number axis indicates the band gap. The height of the theoretical curve has been fixed by matching to the experimental curve at the top of the broad peak in the acoustic band. The force constant Δf was fixed by the local mode frequency; Δg was used as an adjustable parameter. (See Fig. 1.) The "tetragonal" resonance predicted in the gap by TK (dashed vertical line) has moved into the acoustic band to 78.5 cm^{-1}; and the "breathing" resonance which they predicted at 125 cm^{-1} has moved to 108 cm^{-1}, improving qualitative agreement with experiment. (Background has not been subtracted from the experimental results.)

to $I_{\gamma\gamma'}(\omega^2)$ was calculated bin-by-bin. The result is six histograms which approximate the functions $I_{\gamma\gamma'}(\omega^2)$. The functions $R_{\gamma\gamma'}(\omega^2)$ were computed from these using the Cauchy integral of Eq. (27).

V. RESULTS AND DISCUSSION

Results for the cases of KBr and KI have been plotted in Figs. 4 and 5, with the corresponding experimental and theoretical curves of Timusk and Klein.[9,11]

[19] G. A. Dolling, R. A. Cowley, C. Schittenhelm, and I. M. Thorson, Phys. Rev. **147**, 577 (1966).

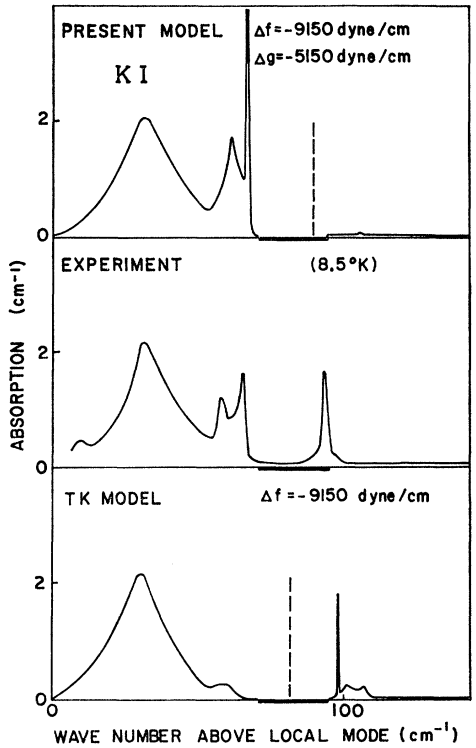

FIG. 5. The results of the present calculation for KI are compared with experimental and theoretical results of Timusk and Klein (Ref. 10). See caption of Fig. 4. TK have observed a resonance in the gap at 93.5 cm^{-1}, and their model predicts (dashed vertical line on bottom curve) that it is due to a "tetragonal" resonance of the H^- ion with its nearest neighbors. In the extended model, this resonance has moved into the acoustic band to 67 cm^{-1}, improving agreement in this region, and the gap mode is now shown (dashed vertical line on top curve) to be due to a "breathing" resonance (which occurred in the optical band in the TK model).

The present calculation shown in the same figure shows qualitatively improved agreement with experiment.

The spike predicted in the gap by TK has moved down to provide a sharp in-band resonance at the top of the acoustic band. This corresponds to the peak actually observed at this energy in both crystals.

The breathing mode resonance predicted by TK in the optical band has also moved down—to the lower edge of the band for KBr, and into the gap for KI. This feature accords with the bump experimentally observed at the lower edge of the optical branch in KBr, as well as with the spike observed in the gap in KI. Note that the introduction of the new force constant change has not affected the broad peak in the acoustic branch.

It therefore seems that no major qualitative discrepancies remain between the experimental curves and the theoretical prediction. All the significant peaks in the experimental curves have now been accounted for. Moreover, understanding of the features of these curves is measurably improved. For example, the spike which occurs in the gap for KI is now predicted to arise from

coupling of the H^--ion vibration to a breathing motion of its neighbors. This prediction is accessible to experimental verification by studying the splitting of the sharp peaks under stress.

It must be emphasized, however, that the improved agreement has been achieved at the expense of introducing an extra parameter. Even with this parameter the exact positions of the peaks are not perfectly predicted, and, with the exception of the broad peak in the acoustic band, all predicted peaks appear to be stronger and sharper than the experimental peaks. The most probable explanation of these two discrepancies is that anharmonic shifting and broadening of the lattice modes has not been taken into account. If anharmonic shifting is taken into account, the shell-model frequencies of the perfect lattice must be corrected to the temperature of the present experiments. If anharmonic broadening is taken into account, the Green's-function matrix elements will have (in the diagonal representation) imaginary parts which are Lorentzians of finite width.[20] The sharpest peak possible in the sideband spectrum will be such a Lorentzian peak. The broadening of the peak actually observed in the gap in KI, therefore, provides an estimate of the order of magnitude of the anharmonic broadening. An anharmonic effect of this order will cause noticeable broadening of the sharp peaks predicted in the acoustic band as well. The detailed nature of anharmonic effects on the sideband spectrum is currently under investigation.

[20] A. A. Maradudin and A. E. Fein, Phys. Rev. **128**, 2589 (1962).

The sharpness of the tetragonal resonance in the acoustic band may be initially surprising, since the density of states for the perfect crystal is not small at this frequency. However, the sharpness of this resonance is (in the harmonic approximation) determined solely by the quantity D_{EI}, which is just the density of states for modes having tetragonal symmetry about the position of the H^- ion. This quantity is small for modes near the top of the acoustic band.

The improvement in agreement with experiment of the present model has come about because of the "softening" of the environment of the H^- ion, which has lowered the frequencies of all resonances. It may be that an overestimate of the quantity Δg has resulted from neglect of other force-constant changes. Within the harmonic approximation, however, the agreement of the present model with experiment seems adequate.

In summary, the present calculation has significantly improved qualitative understanding of the existing infrared absorption data in KBr and KI. When anharmonic effects are taken into account, a quantitatively satisfactory theory of the sideband shape can be expected.

ACKNOWLEDGMENTS

The authors are indebted to Professor J. P. Carbotte and Professor M. V. Klein for valuable discussion. Acknowledgment is also made to the Chalk River group, whose shell-model data have been used in these calculations.